

## Stopping power for low-velocity Mg ions in Si, Ge, and GaAs

K. Arstila, J. Keinonen, P. Tikkanen, and A. Kuronen

*Accelerator Laboratory, University of Helsinki, Hämeentie 100, SF-00550 Helsinki, Finland*

(Received 16 November 1990; revised manuscript received 21 February 1991)

The stopping power for  $^{26}\text{Mg}$  ions in Si, Ge, and GaAs has been studied in the energy region 0–0.8 MeV/nucleon by application of the inverted Doppler-shift-attenuation analysis method. Compared to the commonly used empirical electronic stopping power by Ziegler, Biersack, and Littmark, significant deviations and a different velocity dependence were obtained. The electronic stopping power was determined to an accuracy of  $\pm 5\%$ . The experimental nuclear stopping power was taken into account in the deduction of the electronic stopping power.

### I. INTRODUCTION

In recent years, heavy-ion implantation of semiconductors at MeV energies has become a technique in the very-large-scale-integration (VLSI) technology.<sup>1–4</sup> Knowledge of the depth distributions of implants and damage requires knowledge of the stopping power of semiconductors for heavy ions.

Experimental information on the electronic stopping power has been used by Ziegler, Biersack, and Littmark<sup>5</sup> to construct an empirical model (ZBL) on the basis of the Brandt-Kitagawa theory.<sup>6</sup> This empirical model is now commonly used in all cases where the electronic stopping power is needed to predict concentration distributions of implanted atoms or interpret results of various measurements with heavy-ion beams. Due to experimental difficulties and difficulties in taking into account a realistic nuclear stopping power, there are very few experimental data available in the literature that could be used to test the empirical electronic stopping power in the low-velocity region  $v \leq 2v_0$  ( $v_0 \approx c/137$  is the Bohr velocity). Without an experimental confirmation the validity of the ZBL model is ambiguous.

To verify predictions of the ZBL stopping power for concentration distributions, range distributions of MeV Li, B, and N ions implanted into Si and Ge have very recently been studied by Fink and co-workers.<sup>7–10</sup> The results showed that for ion implantation into Si and Ge up to a few MeV, the range profiles can be reproduced by the use of the ZBL model. In a recent study of MeV Si ions in Si,<sup>11</sup> the range values indicated the electronic stopping power to be about 10% lower than predicted by ZBL.

The aim of this work was to test the empirical electronic stopping power of the basic semiconductor materials Si, Ge, and GaAs for  $^{26}\text{Mg}$  ions. This work is a part of our systematic studies on stopping power for low-velocity ( $v \leq 2v_0$ ) heavy ions in matter.<sup>12–14</sup> In these studies a technique of nuclear physics, the inverted Doppler-shift-attenuation analysis (IDSAA), has been applied. In stopping power measurements, the use of IDSAA is also a

complementary technique to those (Rutherford backscattering spectrometry, nuclear reaction analysis, spreading resistance, secondary ion mass spectrometry, thermal neutron depth profiling, and optical reflectivity measurements) used in the previous studies to profile the distributions of implants.<sup>7–11</sup>

### II. EXPERIMENTAL PROCEDURE

The targets were prepared by implanting  $3 \times 10^{17}$  40-keV  $^{12}\text{C}^+$  ions  $\text{cm}^{-2}$  into single crystal semiconductor materials Si, Ge, and GaAs at the isotope separator of the laboratory. Also a very low-density carbon target on a Si backing was prepared.<sup>15</sup>

In the Doppler-shift-attenuation (DSA) measurements, the velocity of recoiling nuclei at the moment of the  $\gamma$ -ray emission depends on the stopping power of the slowing-down material. The line shape of a  $\gamma$  peak in the  $\gamma$ -ray spectrum shows the velocity distribution of the recoiling nuclei at the moment of the  $\gamma$ -ray emission. In IDSAA the stopping power is deduced by the use of a known lifetime value. The well-established mean lifetime of the first excited state in  $^{26}\text{Mg}$  ( $\tau = 661 \pm 28$  fs,  $E_x = 1809$  keV, Refs. 16 and 17) is a good standard for the study of the stopping power.

The recoiling Mg ions and the excitation of the 1.81-MeV  $^{26}\text{Mg}$  nuclear level were produced in the reaction  $^{12}\text{C}(^{16}\text{O}, 2p)^{26}\text{Mg}$ . Beam energy of 20.0 MeV was chosen to obtain the initial mean velocity of  $4.1v_0$  of the compound  $^{28}\text{Si}$  nuclei. The initial velocity distribution of the recoiling  $^{26}\text{Mg}$  ions was determined experimentally by the use of the low-density carbon target.<sup>15</sup>

The  $\text{O}^{5+}$  beams of 0.5 – 1.5  $\mu\text{A}$  were supplied by the tandem accelerator EGP-10-II of the laboratory. The ion beam was focused to a  $3 \times 3$  mm<sup>2</sup> spot on the target. A vacuum better than 1  $\mu\text{Pa}$  in the target chamber was used to minimize carbon buildup on the target surface during the measurements.

The  $\gamma$ -ray spectra were measured with both the implanted  $^{12}\text{C}$  and the low-density carbon targets and stored in an 8K memory. The dispersion was 1.0 keV/channel. The  $\gamma$  rays were detected with a coaxial

ally drifted high-purity-germanium detector with an efficiency of 40%. The energy resolution [full width at half maximum (FWHM)] of the detection system was 2.0 keV at  $E_\gamma = 1.3$  MeV. The stability of the spectrometer was controlled during the measurements with a  $^{56}\text{Co}$   $\gamma$ -ray source and a  $^{40}\text{K}$  laboratory background. The detector was located at the angle of  $0^\circ$  to the beam direction and subtended a solid angle of 700 msr. The detector axis was aligned to the beam direction. The count rate due to the low-energy  $\gamma$  rays and x rays was limited by the use of a 4-mm lead absorber between the target and the detector. The energy and efficiency calibration of the  $\gamma$ -ray detector was done with  $^{56}\text{Co}$  and  $^{152}\text{Eu}$  sources<sup>18,19</sup> placed in the target position.

The Doppler-broadened  $\gamma$ -ray line shapes were first corrected for the background. This was done by subtracting a shaped background which had the form of a running integral matched to the mean background levels below and above the peak. In the  $\gamma$ -ray spectra observed with the Si backing, the 1.81-MeV  $\gamma$ -ray line shape was also corrected for the contamination due to the 1.78 MeV  $\gamma$ -ray line shape of  $^{28}\text{Si}$  produced in the Coulomb excitation. This was done by subtracting from the spectra a

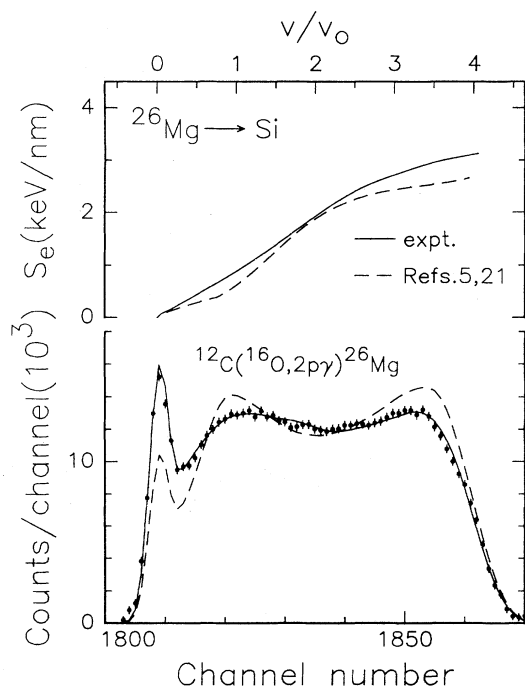


FIG. 1. Portion of a  $\gamma$ -ray spectrum illustrating the slowing down of  $^{26}\text{Mg}$  ions in Si. The 1.81-MeV  $^{26}\text{Mg}$   $\gamma$ -ray peak was measured at  $E(^{16}\text{O}) = 20.0$  MeV to obtain the velocity range of  $(4.1-0)v_0$  for the  $^{26}\text{Mg}$  ions. The solid line shows the line shape obtained in the computer simulation with the adjusted electronic stopping power. The dashed line illustrates the line shape for the empirical electronic stopping power (Refs. 5 and 21). The experimental (solid line) and empirical (dashed line) electronic stopping power ( $S_e$ , in keV/nm) of Si for  $^{26}\text{Mg}$  ions is shown in the upper part of the figure as a function of the ion velocity (in units of Bohr velocity  $v_0$ ).

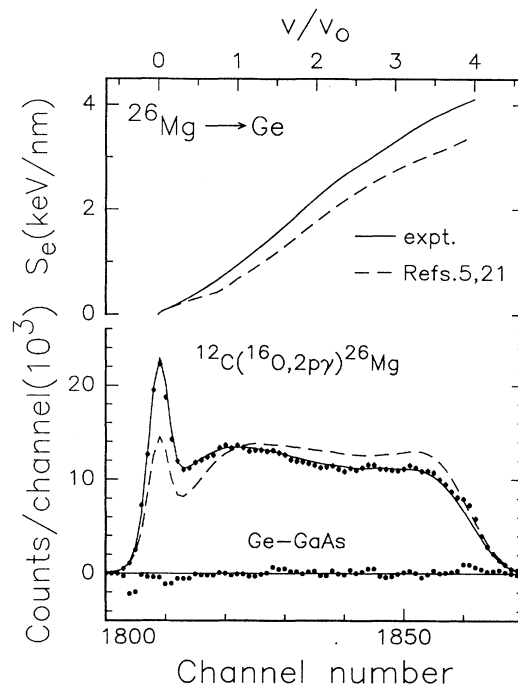


FIG. 2. As for Fig. 1, but for the Ge backing. The difference between the line shapes observed with the Ge and GaAs substrates is shown in the lower part of the figure.

$\gamma$ -ray spectrum observed with the Si backing without the  $^{12}\text{C}$  implants. The experimental line shape was then corrected for the change of the detector efficiency in the energy region of the peak. Experimental  $\gamma$ -ray line shapes corrected for these effects are illustrated in Figs. 1 and 2 for Si and Ge, respectively. A line shape identical to that obtained for Ge was obtained for GaAs.

### III. RESULTS

For the tests of the semiempirical stopping power values,<sup>5</sup> the Doppler-broadened 1.81-MeV  $\gamma$ -ray line shape corresponding to the velocity spectrum of the recoiling  $^{26}\text{Mg}$  ions at the moment of the  $\gamma$ -ray emission was produced by computer simulations. The line shape of the  $\gamma$ -ray peak depends mainly on the stopping power of the slowing-down materials and the lifetime ( $\tau = 661 \pm 28$  fs) of the 1.81-MeV  $^{26}\text{Mg}$  level. The measured line shapes were also affected by other effects which were taken into account in the simulations and are first discussed in the following.

The initial velocity distribution of the recoiling Mg ions obtained in the measurements with the low-density carbon target was taken into account in the simulations of the  $\gamma$ -ray line shapes. The measured velocity distribution was reproduced with a computer code written to simulate the effect of the emission of two protons on the recoil velocity of  $^{26}\text{Mg}$ .

At the bombarding energy used, the measured  $\gamma$ -ray spectra showed that no corrections for the delayed feed-

ings from higher excited states<sup>16</sup> to the 1.81-MeV <sup>26</sup>Mg state were needed in the simulations. The simulated line shapes were deduced for the direct prompt population of the 1.81-MeV state.

The effect of the finite size of the  $\gamma$ -ray detector and the measured dependence of the detector efficiency on the angle between the  $\gamma$ -ray emission and the symmetry axis of the detector were taken into account in the simulations. The Doppler shift of an emitted  $\gamma$ -ray was calculated up to the second order in the velocity of the recoiling ions.

The simulated  $\gamma$ -ray line shapes were convoluted with the experimental line shape, measured with a standard radioactive source, to account for the finite-energy resolution of the detector. The intensity of the simulated peak was required to be equal to the intensity of the experimental peak in the final  $\chi^2$  fit of the line shapes.

The stopping power of the slowing-down materials for the recoiling <sup>26</sup>Mg ions was described according to the following equation:

$$\left(\frac{dE}{dx}\right)_{\text{corr}} = f_n \left(\frac{dE}{dx}\right)_n + f_e \left(\frac{dE}{dx}\right)_e. \quad (1)$$

The uncorrected nuclear stopping power  $(dE/dx)_n$  was derived by calculating the scattering angles of the recoiling ions directly from the classical scattering integral. The interatomic interaction was derived from the universal interatomic potential (ZBL).<sup>5</sup> The effect of the crystalline structure on the slowing-down was taken into account by the correction factor  $f_n$  which accounts for the reduction of the nuclear stopping power due to the channeling of the recoiling atoms. The adopted value of  $f_n = 0.95 \pm 0.05$  was based on stopping power measurements at low ( $v \leq v_0$ ) velocities.<sup>20</sup>

In the simulation of the 1.81-MeV  $\gamma$ -ray line shape, the uncorrected electronic stopping power  $(dE/dx)_e$  was first calculated in the framework of the empirical model<sup>5</sup> by the use of the TRIM-89 computer code.<sup>21</sup> It was observed that the electronic energy loss is significantly higher and its velocity dependence different than predicted by the empirical model (ZBL-89) (see Figs. 1 and 2). Succeedingly, it was obtained that there were no values of the scaling factor  $f_e$  which could be adequate for the description of the measured line shapes. In order to reproduce the experimental line shapes, the electronic stopping power was deduced by an iterative procedure. The procedure was initialized with the ZBL-89 values. The difference between the simulated and measured line shape was used to correct the stopping power at each velocity represented by the channel number. The iterative procedure was continued until the minimum value of  $\chi^2$  was obtained in the fit of the line shapes.

The simulated  $\gamma$ -ray line shapes are illustrated in Figs. 1 and 2 for the stopping power deduced in this work. The stopping power values are given in Table I. Figures 1 and 2 show also the comparison between the present (expt.) and empirical<sup>5,21</sup> electronic stopping power of Si and Ge for <sup>26</sup>Mg ions, respectively.

TABLE I. Results for the electronic stopping power [in MeV/(mg cm<sup>-2</sup>)] for <sup>26</sup>Mg ions in Si, Ge, and GaAs. The absolute uncertainty is  $\pm 5\%$ . Corrections for the nuclear stopping power have been applied in the deduction of the given values.

| $v/v_0$ | Si    | Ge   | GaAs |
|---------|-------|------|------|
| 0.2     | 0.79  | 0.31 | 0.31 |
| 0.4     | 1.51  | 0.61 | 0.61 |
| 0.6     | 2.26  | 0.95 | 0.95 |
| 0.8     | 3.02  | 1.33 | 1.33 |
| 1.0     | 3.81  | 1.75 | 1.75 |
| 1.2     | 4.64  | 2.20 | 2.20 |
| 1.4     | 5.53  | 2.67 | 2.67 |
| 1.6     | 6.45  | 3.15 | 3.15 |
| 1.8     | 7.38  | 3.65 | 3.65 |
| 2.0     | 8.32  | 4.15 | 4.15 |
| 2.2     | 9.21  | 4.63 | 4.63 |
| 2.4     | 10.00 | 5.06 | 5.06 |
| 2.6     | 10.68 | 5.43 | 5.43 |
| 2.8     | 11.24 | 5.79 | 5.79 |
| 3.0     | 11.73 | 6.16 | 6.16 |
| 3.2     | 12.18 | 6.55 | 6.55 |
| 3.4     | 12.59 | 6.90 | 6.90 |
| 3.6     | 12.92 | 7.19 | 7.19 |
| 3.8     | 13.18 | 7.45 | 7.45 |
| 4.0     | 13.42 | 7.70 | 7.70 |

The uncertainty  $\pm 5\%$  of the given stopping power arises from the uncertainty of the mean lifetime of the 1.81-MeV <sup>26</sup>Mg state, the uncertainties due to the corrections of the simulated line shapes, and the statistical uncertainties. The uncertainty of the nuclear stopping power correction was observed to have a negligible effect on the uncertainty of the electronic stopping power. The present stopping power of Ge supersedes our earlier results<sup>14</sup> based on data with considerably lower experimental intensity of the  $\gamma$ -ray line shape than measured in this work. In the earlier work the stopping power was obtained by scaling the empirical stopping power.<sup>5</sup> The present method, explained above, resulted in a more accurate description of the  $\gamma$ -ray line shapes.

For the semiconductor band-gap targets Si and Ge the velocity dependence of the stopping power at low velocities has been assumed in the semiempirical model to be  $(v/v_0)^{0.75}$ . The maximum values of this velocity region have been taken to be  $0.75v_0$  for Si and  $0.76v_0$  for Ge.<sup>5</sup> The present stopping power measurements indicate that such regions are not detectable or the values of the maximum velocities are considerably lower than used in the empirical model, see Figs. 1 and 2.

The deduced experimental stopping power of GaAs was identical to that obtained for Ge (see Fig. 2). If we assume that Bragg's additivity rule<sup>22</sup> is valid, the result indicates that there are similar errors in the semiempirical stopping power values of Ga and As as obtained here for Ge.

## IV. SUMMARY

The empirical electronic stopping power (ZBL-89) (Refs. 5 and 21) has been tested to an accuracy of  $\pm 5\%$  for  $(0-4)v_0$  Mg ions in Si, Ge, and GaAs by application of the IDSAA method in conjunction with the well-established nuclear lifetime and nuclear stopping powers. The results show greater than 10% deviations of the

stopping powers and their velocity dependencies from the predictions of the recent parametrization of the empirical model of ZBL.<sup>5</sup>

## ACKNOWLEDGMENT

This work was supported by the Academy of Finland.

- 
- <sup>1</sup>D. Pramanik and A. N. Saxena, Nucl. Instrum. Methods B **10&11**, 493 (1985).  
<sup>2</sup>D. C. Ingram, J. A. Baker, and D. A. Walsh, Nucl. Instrum. Methods B **7&8**, 361 (1985).  
<sup>3</sup>T. Tokyama, Nucl. Instrum. Methods B **19&20**, 299 (1987).  
<sup>4</sup>W. R. Fahrner, J. R. Laschinski, and D. Bräunig, Nucl. Instrum. Methods A **268**, 579 (1988).  
<sup>5</sup>J. F. Ziegler, J. P. Biersack, and U. Littmark, in *The Stopping Power and Ranges of Ions in Matter*, edited by J. F. Ziegler (Pergamon, New York, 1985), Vol. 1.  
<sup>6</sup>W. Brandt and M. Kitagawa, Phys. Rev. B **25**, 5631 (1982).  
<sup>7</sup>M. Behar, M. Weiser, S. Kalbitzer, D. Fink, and P. L. Grande, Nucl. Instrum. Methods B **39**, 22 (1989).  
<sup>8</sup>D. Fink, J. P. Biersack, M. Müller, V. K. Cheng, R. Kassing, K. Masseli, M. Weiser, and S. Kalbitzer, Mater. Sci. Eng. B **2**, 49 (1989).  
<sup>9</sup>D. Fink, J. P. Biersack, H. P. Schölch, M. Weiser, S. Kalbitzer, M. Behar, J. P. DeSouza, F. C. Zawislak, A. Mazzone, and H. Kranz, Radiat. Eff. Defs. **108**, 185 (1989).  
<sup>10</sup>D. Fink, K. Tjan, L. H. Wang, and Y. R. Ma, Radiat. Eff. Defs. **108**, 27 (1989).  
<sup>11</sup>N. Hecking (unpublished).  
<sup>12</sup>J. Keinonen, A. Kuronen, M. Hautala, V. Karttunen, R. Lappalainen, and M. Uhrmacher, Phys. Lett. A **123**, 307 (1987).  
<sup>13</sup>P. Tikkanen, Nucl. Instrum. Methods B **36**, 103 (1989).  
<sup>14</sup>K. Arstila, J. Keinonen, and P. Tikkanen, Phys. Rev. B **41**, 6117 (1990).  
<sup>15</sup>P. Tikkanen, J. Keinonen, V. Karttunen, and A. Kuronen, Nucl. Phys. **A456**, 337 (1986).  
<sup>16</sup>P. M. Endt and C. van der Leun, Nucl. Phys. **A310**, 1 (1978).  
<sup>17</sup>B. H. Wildenthal and J. Keinonen (unpublished).  
<sup>18</sup>M. Hautala, A. Anttila, and J. Keinonen, Nucl. Instrum. Methods **150**, 599 (1978).  
<sup>19</sup>C. M. Lederer and V. S. Shirley, *Table of Isotopes*, 7th ed. (Wiley, New York, 1978).  
<sup>20</sup>R. Paltamaa, J. Räsänen, M. Hautala, and A. Anttila, Nucl. Instrum. Methods **218**, 785 (1983).  
<sup>21</sup>J. F. Ziegler and J. P. Biersack, TRIM-89 computer code (private communication).  
<sup>22</sup>W. H. Bragg and R. Kleeman, Philos. Mag. **10**, 318 (1905).